HDAC9 Inhibits Osteoclastogenesis via Mutual Suppression of PPARγ/RANKL Signaling

Zixue Jin, Wei Wei, HoangDinh Huynh, and Yihong Wan

Department of Pharmacology, University of Texas Southwestern Medical Center, Dallas, Texas 75390

Recent studies suggest that the class II histone deacetylase (HDAC)9 plays important roles in physiology such as metabolism and immunity. Here, we report that HDAC9 also controls bone turnover by suppressing osteoclast differentiation and bone resorption. HDAC9 expression is down-regulated during osteoclastogenesis. Ex vivo osteoclast differentiation is accelerated by HDAC9 deletion but diminished by HDAC9 overexpression. HDAC9 knockout mice exhibit elevated bone resorption and lower bone mass. Bone marrow transplantation reveal that the osteoclastogenic defects are intrinsic to the hematopoietic lineage, because the excessive bone resorption phenotype can be conferred in wild-type (WT) mice receiving HDAC9-null bone marrow, and rescued in HDAC9-null mice receiving WT bone marrow. Mechanistically, HDAC9 forms a negative regulatory loop with peroxisome proliferator-activated receptor gamma (PPARg) and receptor activator of nuclear factor kappa-B ligand (RANKL) signaling. On one hand, PPARγ and nuclear factor κB suppress HDAC9 expression, on the other hand, HDAC9 inhibits PPARγ activity in synergy with silencing mediator of retinoic acid and thyroid hormone receptors (SMRT)/NCoR corepressors. These findings identify HDAC9 as a novel, important and physiologically relevant modulator of bone remodeling and skeletal homeostasis. (***Molecular Endocrinology*** **29: 730–738, 2015)**

Skeletal maintenance relies on both osteoclast-mediated bone resorption and osteoblast-mediated bone formation. Osteoclast differentiation from hematopoietic macrophage precursors is mainly dependent on 2 critical cytokines: macrophage colony-stimulating factor (MCSF) and receptor activator of nuclear factor κB (NFκB) ligand (RANKL) (1, 2). This osteoclastogenesis process can be enhanced by other signaling pathways such as the nuclear receptor transcription factor PPARγ and its synthetic agonist rosiglitazone, a widely used drug for insulin resistance and type 2 diabetes (3, 4). Osteoclast overabundance is associated with several bone degenerative diseases such as osteoporosis, inflammatory arthritis, multiple myeloma, and cancers metastasis to bone, whereas osteoclast deficiency may lead to rare diseases such as osteopetrosis (5, 6).

Histone acetyltransferases (HATs) and histone deacetylases (HDACs) posttranslationally modify not only histones but also other proteins by adding or removing acetyl groups, thereby acting as a switch of their structures and functions. For example, histone hyperacetylation often causes a relaxed chromatin structure that facilitates transcription factors binding to DNA and activate transcription, whereas histone hypoacetylation often induces a compact structure, so that transcription factors are excluded to inhibit transcription (7). In the absence of ligand, nuclear receptor family of transcription factors associate with corepressors such as SMRT and NCoR to recruit HDACs and prevent transcription of their target genes; upon ligand binding, they dissociate from corepressors and partner with coactivators such as peroxisome proliferator-activated receptor gamma coactivator 1α/β and steroid receptor coactivators to bring in histone acetyltransferases such as CREB-binding protein/p300 and activate transcription (8).

HDACs are evolutionarily conserved. They are divided into 4 classes based on function and DNA sequence sim-

Abbreviations: BMD, bone mineral density; BMT, bone marrow transplantation; BrdU, 5-bromo-2′-deoxyuridine; BS, bone surface; BV/TV, bone volume to tissue volume ratio; CMV-bgal, cytomegalovirus-beta galactosidase; CTX-1, C-terminal telopeptide fragments of the type I collagen; HAT, histone acetyltransferase; HDAC, histone deacetylase; HDAC9-KO, HDAC9 knockout; MCSF, macrophage colony-stimulating factor; uCT, micro-Computed Tomography; NCoR, nuclear receptor corepressor; NFκB, nuclear factor κB; P1NP, N-terminal propeptide of type I procollagen; PPAR, peroxisome proliferator-activated receptor; PPRE-luc, PPAR response element-luciferase; RANKL, receptor activator of NFκB ligand; RXR, retinoid X receptor; SMRT, silencing mediator of retinoic acid and thyroid hormone receptors; SMI, structure model index; TRAP, tartrate-resistant acid phosphatase; WT, wild-type.

ISSN Print 0888-8809 ISSN Online 1944-9917
Printed in U.S.A.

Received November 15, 2014. Accepted March 17, 2015.
First Published Online March 20, 2015

ilarity. The classical HDACs have 11 family members that are divided into 3 groups: class I (HDAC1, HDAC2, HDAC3, and HDAC8), class II (IIa subgroup includes HDAC4, HDAC5, HDAC7, and HDAC9; IIb subgroup includes HDAC6 and HDAC10), and class IV (HDAC11) (9). Class III HDACs are an atypical group that are also known as sirtuins (9). HDAC inhibitors have been long recognized as promising drugs for cancer, neurodegeneration, and cognitive disorders (10, 11). Therefore, it is pivotal to determine the effects of each HDAC on osteoclasts and bone. This knowledge may uncover certain HDACs modulators as novel treatment for osteoporosis but also reveal potential bone loss side effects of current therapeutic HDAC inhibitors.

HDAC7 and HDAC3 have been shown to regulate osteoclast differentiation in vitro (12). Recently, we have reported HDAC7 as the first HDAC that regulates osteoclastogenesis and bone resorption in vivo (13). In this study, we continued to ask whether other HDAC members also regulate osteoclastogenesis in vivo, and identified HDAC9 as another novel yet critical suppressor of osteoclast development. These findings are timely and important, because an increasing number of reports have demonstrated the crucial roles of HDAC9 in a variety of physiological and disease processes such as T cells and autoimmunity (14), macrophages and atherosclerosis (15), and adipogenesis and metabolic disorders (16, 17). Moreover, a recent genome-wide association study has identified an HDAC9 variant that correlates with large vessel ischemic stroke in human population (18).

Materials and Methods

Mice

HDAC9 knockout (HDAC9-KO) mice on a C57BL/6J background were provided by Dr Eric Olson (19). Mice were fed with standard chow ad libitum and kept on a 12-hour light, 12-hour dark cycle. All experiments were conducted using littermates. Bone marrow transplantation (BMT) was performed as described (4, 20). Briefly, bone marrow cells from 2-month-old donor (WT or HDAC9-KO) were iv transplanted into 2-month-old recipients (WT or HDAC9-KO) that were irradiated at lethal dose (1000 R); the mice were analyzed 3 months after transplantation. Sample size estimate was based on power analyses performed using SAS 9.3 TS X64_7PRO platform at the University of Texas Southwestern Medical Center Biostatistics Core. With the observed group differences and the relatively small variation of the in vivo measurements, n = 4 and n = 3 will provide more than 90% and more than 80% power at type I error rate of 0.05 (2-sided test), respectively. All protocols for mouse experiments were approved by the Institutional Animal Care and Use Committee of University of Texas Southwestern Medical Center.

Bone analyses

μCT was performed to evaluate bone volume and architecture using a Scanco μCT-35 instrument (SCANCO Medical) as previously described (20). As a bone resorption marker, serum C-terminal telopeptide fragments of the type I collagen (CTX-1) was measured with the RatLaps Enzyme Immunoassay kit (Immunodiagnostic Systems). As a bone formation marker, serum N-terminal propeptide of type I procollagen (P1NP) was measured with the Rat/Mouse P1NP EIA kit (Immunodiagnostic Systems).

Ex vivo bone marrow osteoclast differentiation

Osteoclast differentiation from bone marrow cells was performed as previously described (21). Briefly, bone marrow cells were purified through 40-μm cell strainer and cultured in αMEM (Minimum Essential Medium) with MCSF (40 ng/mL; R&D Systems) for 3 days and then differentiated with MCSF (40 ng/mL) and RANKL (100 ng/mL; R&D Systems) for another 3–6 days. RNA was collected on day 6 (3 day after RANKL stimulation), and tartrate-resistant acid phosphatase (TRAP) staining was performed on day 9 (6 day after RANKL stimulation). For osteoclast resorptive function analyses, bone marrow osteoclast differentiation was conducted in OsteoAssay bone plates (Lonza), and osteoclast activity was quantified as calcium release from bone into culture medium using CalciFluo ELISA assay (Lonza). Expression of differentiation markers was quantified by reverse transcription-quantitative polymerase chain reaction in triplicates and normalized by the ribosomal gene L19.

Osteoclast precursor proliferation assay

Osteoclast precursor proliferation was quantified using a BrdU Cell Proliferation Assay kit (GE Healthcare Life Sciences) (22, 23). Mouse bone marrow cells were treated with MCSF (40 ng/mL) for 1 or 3 days. The cells were MCSF starved for 6 hours and then restimulated with MCSF for 4 hours to induce S phase, during which BrdU was provided in the culture medium. Cell proliferation was quantified as BrdU incorporation using the BrdU ELISA assay in the kit.

Transient transfection and reporter analysis

To quantify PPARγ transcriptional activity, CV-1 cells were cotransfected with PPRE-luc reporter and expression vectors for PPARγ, RXRα, HDAC9, NCoR, and/or SMRT or vector control, as well as a CMV-β-gal reporter as internal control. To quantify HDAC9 promoter activity, HEK293 cells were cotransfected with a luciferase reporter driven by a 921-bp mouse HDAC9 promoter fragment (24) and expression vectors for PPARγ, RXRα, and/or p65 or vector control, as well as a CMV-β-gal reporter as internal control. All transfections were conducted with FuGENE HD (Roche) at n = 6 per condition, luciferase output was analyzed 48 hours after transfection and normalized by β-gal output. Each experiment was repeated at least 3 times, and representative results are shown. For primary cells transfection, bone marrow cells were purified through 40-μm cell strainer and cultured overnight with MCSF (40 ng/mL) and then transfected with HDAC9 expression plasmid or vector control using FuGENE HD. The cells were then cultured for 3 more days in MCSF (40 ng/mL), followed by 3 days in

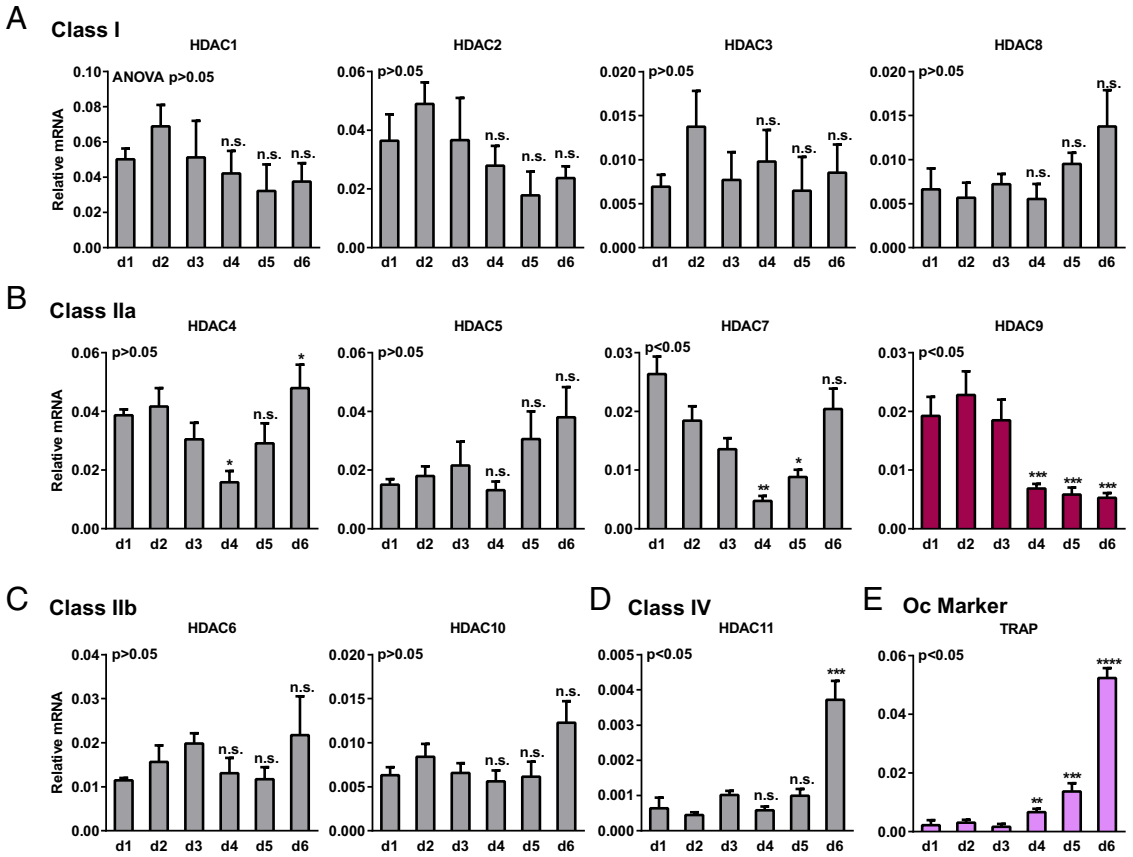

Figure 1. Expression of HDACs during a time course of osteoclastogenesis. Bone marrow cells from WT mice were cultured in 40-ng/mL MCSF during the first 3 days (d1–d3) to stimulate osteoclast precursor proliferation and then cultured in 40-ng/mL MCSF and 100-ng/mL RANKL for the last 3 days (d4–d6) to induce osteoclast differentiation. A–D, Expression of each member in the classic HDAC classes was quantified on each day by RT-QPCR (n = 3). A, Class I. B, Class IIa. C, Class IIb. D, Class IV. E, Expression of a representative osteoclast differentiation marker (n = 3). * and n.s. compare expression on d4, d5, or d6 (after RANKL treatment) with the expression on d3 (before RANKL treatment). Error bars, SD.

MCSF (40 ng/mL) and RANKL (100 ng/mL). Effects on osteoclast marker expression was analyzed by RT-qPCR.

Statistical analyses

Statistical analyses for more than 2 groups were performed by ANOVA and the post hoc Tukey pairwise comparisons. All other statistical analyses were performed with Student's *t* test. Results are represented as mean ± SD unless noted otherwise. The *P* values were designated as: *, $P < .05$; **, $P < .01$; ***, $P < .005$; ****, $P < .001$; n.s., nonsignificant ($P > .05$).

Results

HDAC9 is down-regulated during osteoclast differentiation

We examined the expression of all the classic HDAC members during a time course of mouse bone marrow osteoclast differentiation. All HDAC members in class I, II, and IV were expressed in both proliferating osteoclast precursors (first 3 d with MCSF treatment) and differentiating osteoclasts (later 3 d with MCSF plus RANKL treatment) (Figure 1, A–D). Among these HDACs, the expression of HDAC9 was one of the most significantly down-regulated upon RANKL stimulation (day 4 vs day 3) (Figure 1B). Furthermore, HDAC9 expression remained low during osteoclast differentiation (d4–d6) (Figure 1B). As expected, the expression of osteoclast differentiation markers such as TRAP was significantly increased upon RANKL stimulation (Figure 1E). These results suggest that HDAC9 may negatively regulate osteoclast differentiation.

HDAC9-KO mice exhibit high bone resorption and low bone mass

To determine whether HDAC9 is a physiologically significant regulator of osteoclastogenesis and bone resorption, we examined the skeletal phenotype in HDAC9-KO mice. As described in previous study (19), HDAC9−/− mice appeared overtly normal at 3 months of age without significant differences in body weight or tibiae length (data not shown). Interestingly, μCT analysis revealed that HDAC9-KO mice exhibited a lower bone mass compared with WT control mice (Figure 2A). Quantification

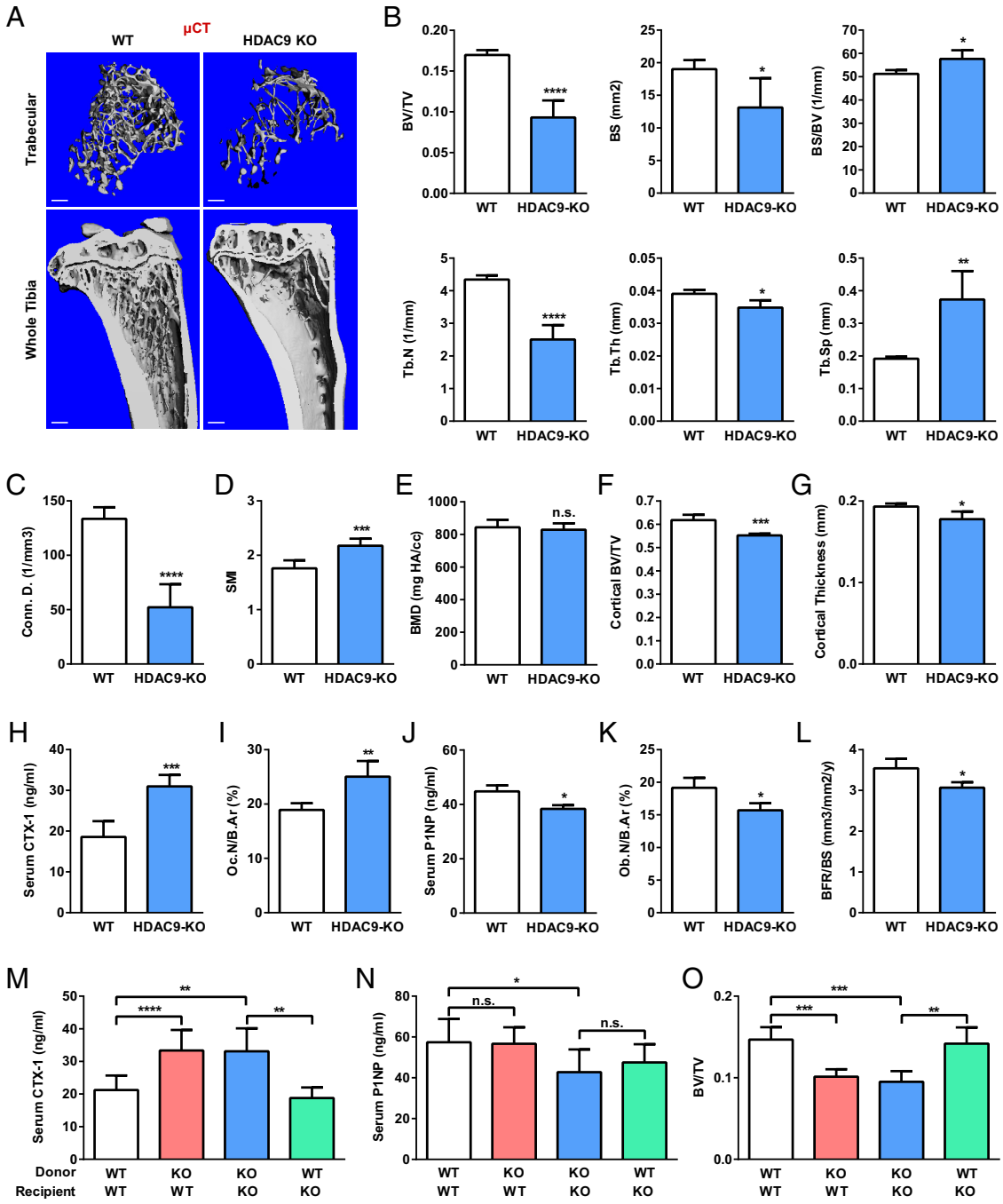

Figure 2. HDAC9-KO mice exhibit elevated bone resorption and low bone mass. A–E, HDAC9-KO mice displayed a low-bone-mass phenotype. Tibiae from HDAC9-KO mice or WT controls (3-month-old, male; n = 4) were analyzed by μCT. A, Representative images of the trabecular bone of the tibial metaphysis (top) (scale bar, 10 μm) and the entire proximal tibia (bottom) (scale bar, 1 mm). B–G, Quantification of trabecular bone volume and architecture. B, BV/TV, BS, BS to bone volume ratio (BS/BV), trabecular number (Tb.N), trabecular thickness (Tb.Th), and trabecular separation (Tb.Sp). C, Connectivity density (Conn.D.). D, SMI. E, BMD. F, Cortical bone BV/TV. G, Cortical thickness. H and I, Serum CTX-1 bone resorption marker (H) and osteoclast number (I) were increased (3-month-old, male; n = 4). B.Ar, bone area. J–L, Serum P1NP bone formation marker (J), osteoblast number (K) and bone formation rate (BFR) (L) were decreased (3-month-old, male; n = 4). M–O, BMT was sufficient to confer HDAC9 regulation of bone resorption, but not bone formation. WT recipient mice (2-month-old, female; n = 8) were irradiated and transplanted with bone marrow from WT or HDAC9-KO donor mice (2-month-old, female); HDAC9-KO recipient mice (2-month-old, female; n = 4) were irradiated and transplanted with bone marrow from HDAC9-KO or WT donor mice (2-month-old, female). Serum CTX-1 bone resorption marker (M), serum P1NP bone formation marker (N), and BV/TV by μCT (O) were analyzed 3 months later. Error bars, SD.

of trabecular bone parameters revealed 45% less bone volume to tissue volume ratio (BV/TV), 31% less bone surface (BS), 13% greater BS to bone volume ratio, 42% less trabecular number, 11% less trabecular thickness, and 95% greater trabecular separation (Figure 2B). This resulted in a 61% decrease in connectivity density (Figure

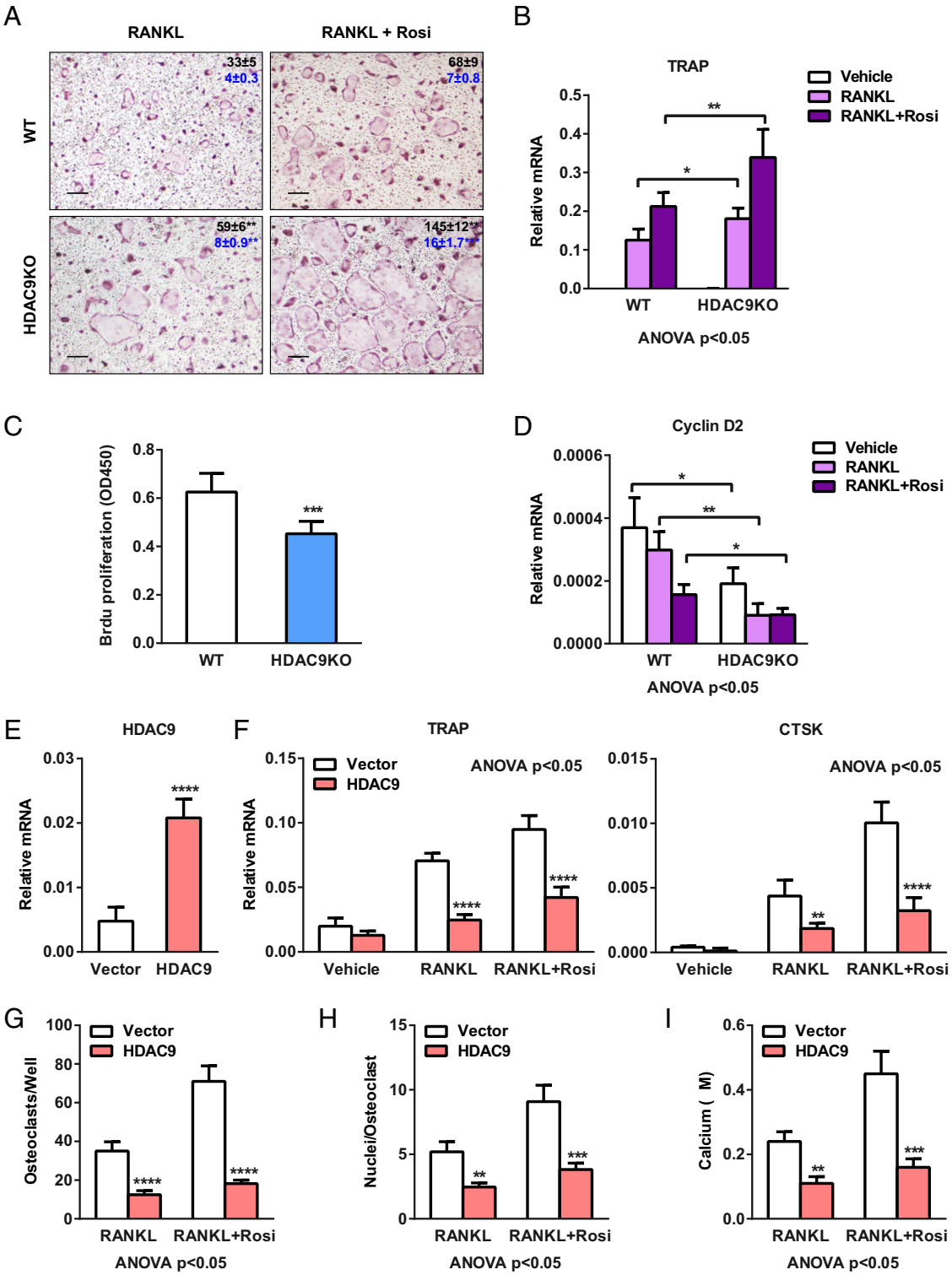

Figure 3. HDAC9 suppresses osteoclastogenesis. A and B, HDAC9 deletion enhances RANKL-induced and rosiglitazone (rosi)-stimulated osteoclast differentiation. Bone marrow cells from HDAC9-KO mice or WT controls were differentiated into osteoclasts with MCSF (d 1–6) and RANKL (d 4–6) in the absence or presence of rosi (d 1–6). A, Representative images of TRAP-stained osteoclast differentiation cultures. Mature osteoclasts were identified as multinucleated TRAP$^+$ (purple) cells. Scale bar, 25 μm. Quantifications for osteoclasts per well (top, black; n = 6) and nuclei per osteoclast (bottom, blue; n = 30) are shown by the numbers in the panels; * compares WT with KO under the same treatment condition. B, Expression of osteoclast differentiation marker TRAP on day 6 (n = 3). C and D, HDAC9 deletion inhibits osteoclast precursor proliferation. C, BrdU incorporation was reduced in HDAC9-KO cultures compared with WT control cultures on day 3 (n = 5). D, Expression of proliferation marker Cyclin D2 was lower in HDAC9-KO cultures compared with WT control cultures on day 6 (n = 3). E–I, HDAC9 overexpression inhibits RANKL-induced and rosi-stimulated osteoclast differentiation. WT bone marrow osteoclast differentiation cultures were transfected with HDAC9 or vector control on day 1. E and F, Expression of HDAC9 (E) as well as osteoclast markers TRAP and CTSK (F) were quantified by RT-QPCR on day 6 (n = 3). G and H, Number of osteoclasts per well (n = 3) (G) and number of nuclei per osteoclast (n = 30) (H) were quantified on day 9. I, Quantification of resorptive activity by calcium release from bone plate into medium (n = 6). Error bars, SD.

2C) and a 24% increase in the structure model index (SMI), which quantifies the three-dimensional structure for the relative amount of plates (SMI = 0, strong bone) and rods (SMI = 3, fragile bone) (Figure 2D). Bone mineral density (BMD) was not significantly altered (Figure 2E). Moreover, HDAC9-KO mice also displayed a significantly decreased cortical bone BV/TV (Figure 2F) and cortical thickness (Figure 2G).

Serum bone resorption marker CTX-1 was elevated by 67% in HDAC9-KO mice (Figure 2H), accompanied by an increased osteoclast number (Figure 2I). In contrast, serum bone formation marker P1NP was reduced by 14% in HDAC9-KO mice (Figure 2J), accompanied by a decreased osteoblast number (Figure 2K) and bone formation rate (Figure 2L). These results suggest that the low-bone-mass phenotype in HDAC9-KO mice is mainly caused by

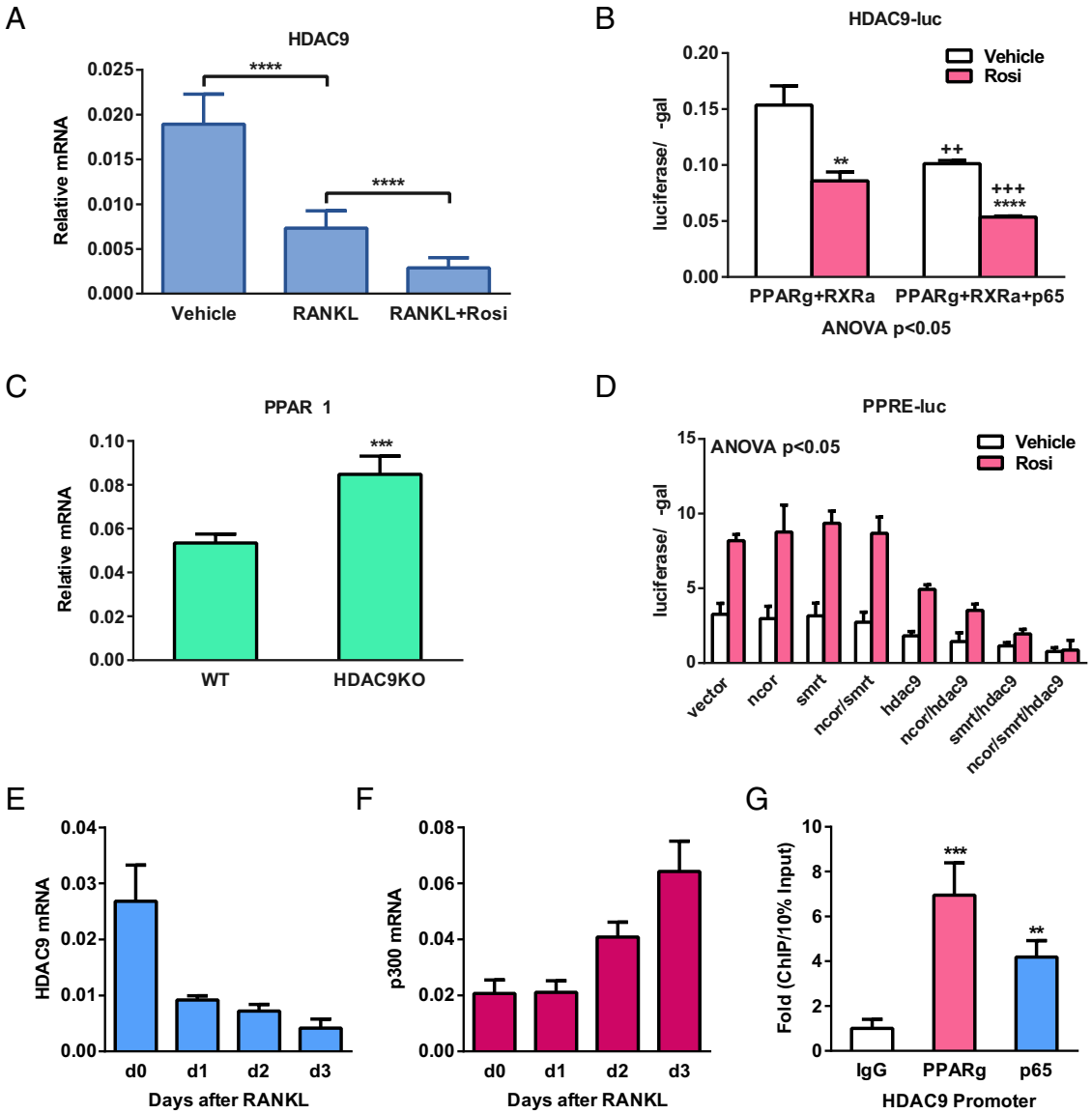

Figure 4. Reciprocal suppression between HDAC9 and PPARγ/RANKL signaling. A and B, PPARγ activation and RANKL signaling inhibit HDAC9 expression. A, HDAC9 expression was decreased by RANKL and further down-regulated by rosiglitazone (Rosi) in osteoclast differentiation cultures (n = 5). B, Readout from a luciferase reporter driven by a 921-bp HDAC9 promoter fragment was reduced by Rosi and further diminished by the NFκB subunit p65. HEK293 cells were transfected with PPARγ, RXRα, and/or p65, together with CMV-β-gal as an internal control, and then treated with Rosi or vehicle control next day; luciferase activity was quantified 24 hours later and normalized by β-gal activity (n = 6). C, HDAC9 inhibits PPARγ1 expression. PPARγ1 expression was elevated in HDAC9-KO bone marrow osteoclast differentiation cultures compared with WT control cultures (n = 5). D, HDAC9 inhibits PPARγ activity together with corepressors SMRT and NCoR. CV-1 cells were cotransfected with PPRE-luc reporter and expression vectors for PPARγ, RXRα, HDAC9, NCoR, and/or SMRT or vector control, as well as a CMV-β-gal reporter as internal control (n = 6). E and F, During RANKL-induced osteoclast differentiation, a decrease in HDAC9 expression (E) was accompanied by an increase in the expression of a HAT p300 (F) (n = 5). G, Chromatin immunoprecipitation (ChIP) analysis of the binding of PPARγ and p65 to HDAC9 promoter in bone marrow osteoclast differentiation cultures on day 6 (n = 4). Error bars, SD.

excessive bone resorption but also contributed by diminished bone formation.

To determine whether the high bone resorption defect was intrinsic to the hematopoietic lineage, we performed BMT (Figure 2, M–O). HDAC9-KO bone marrow was sufficient to confer higher bone resorption in WT recipient mice without altering bone formation. Conversely, WT bone marrow was sufficient to rescue the high bone resorption in HDAC9-KO recipient to a level similar to WT mice without altering bone formation. Moreover, these results showed that female HDAC9-KO mice exhibited a similar phenotype with higher bone resorption, lower bone formation, and reduced bone mass. These data indicate that HDAC9 suppresses bone resorption and osteoclastogenesis in a cell-autonomous manner.

HDAC9 inhibits osteoclast differentiation

We next compared ex vivo osteoclast differentiation from bone marrow cells of HDAC9-KO mice and WT controls. Both RANKL-mediated and rosiglitazone-stimulated osteoclast differentiation was augmented in the HDAC9-KO cultures, shown by the increased number and size of mature osteoclasts (Figure 3A) and the higher expression of osteoclast marker genes such as TRAP (Figure 3B). Moreover, the enhanced differentiation was accompanied by a reduced proliferation of osteoclast precursors, as quantified by BrdU incorporation (Figure 3C) and Cyclin D2 expression (Figure 3D). These results suggest that HDAC9 deletion facilitates a proliferation-to-differentiation switch.

As a complementary gain-of-function strategy, we also examined the effect of HDAC9 overexpression. HDAC9 transfection in WT bone marrow cells significantly increased HDAC9 expression in osteoclast differentiation cultures compared with vector transfected controls (Figure 3E), leading to a significant reduction in RANKL-induced and rosiglitazone-stimulated TRAP expression (Figure 3F). Together, these results indicate that HDAC9 inhibits osteoclast differentiation.

PPARγ and RANKL reduces HDAC9 expression, whereas HDAC9 inhibits PPARγ function

To elucidate the mechanisms for how HDAC9 inhibits osteoclastogenesis, we first examined how HDAC9 is down-regulated during osteoclast differentiation. Compared with MCSF-treated osteoclast precursors, HDAC9 mRNA is decreased by RANKL treatment and further diminished by rosiglitazone treatment (Figure 4A), indicating that RANKL signaling and PPARγ activation inhibits HDAC9 transcription. Indeed, transient transfection and luciferase reporter analyses showed that the activity of HDAC9 promoter was significantly decreased by rosiglitazone treatment in cells transfected with PPARγ and RXRα, as well as by overexpression of the NFκB subunit p65, a RANKL downstream transcription factor (Figure 4B).

Our previous studies have shown the important roles of PPARγ during osteoclastogenesis (4, 25). We found that PPARγ1 mRNA was significantly higher in HDAC9-KO differentiation cultures, indicating that HDAC9 suppresses PPARγ expression (Figure 4C). Furthermore, PPRE-luc reporter assays revealed that

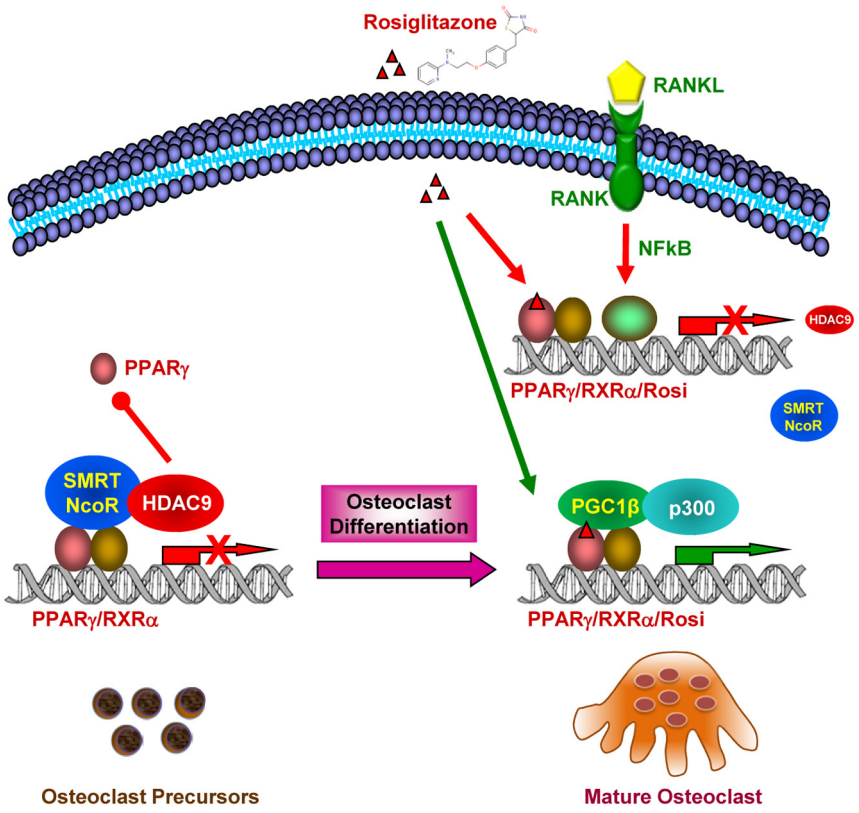

Figure 5. A simplified working model for how a negative feedback loop between HDAC9 and PPARγ/RANKL signaling inhibits osteoclastogenesis. In the absence of RANKL, HDAC9 impedes PPARγ function by both reducing PPARγ expression and suppressing PPARγ activity via corepressors such as SMRT and NCoR; in the presence of RANKL, activation of RANKL downstream transcription factors such as NFκB and activation of PPARγ by its agonist such as rosiglitazone diminishes HDAC9 expression, leading to the recruitment coactivators and HATs, thereby activation of PPARγ target genes. As a result, HDAC9 deletion enhances osteoclast differentiation and bone resorption, leading to low bone mass.

HDAC9 also functions together with corepressors such as NCoR and SMRT to inhibit PPARγ transcriptional activity (Figure 4D). Interestingly, although HDAC9 expression is decreased during a time course of osteoclast differentiation (Figure 4E), the expression of a HAT p300 was increased (Figure 4F). Combined with our previously reported increase of the transcriptional coactivator PGC1β during osteoclast differentiation (26), these results indicate a switch from transcriptional repression state to transcription activation state. In support of the gene expression and transfection analyses, chromatin immunoprecipitation assay showed that both PPARγ and p65 bound to HDAC9 promoter in osteoclast differentiation cultures (Figure 4G). Together, these findings suggest a negative regulatory loop in which PPARγ and RANKL signaling inhibits HDAC9 expression, and HDAC9 in turn inhibits PPARγ expression and activity (Figure 5).

Discussion

In this study, we have identified HDAC9 as a novel yet important negative regulator of osteoclastogenesis and bone resorption. HDAC9 deletion enhances osteoclast differentiation, elevates bone resorption, leading to low bone mass. HDAC9 regulation of osteoclastogenesis is largely intrinsic to the hematopoietic lineage because marrow transplantation-mediated adult onset hematopoietic HDAC9 deficiency is sufficient to increase bone resorption in WT recipients, and vice versa, transplantation with WT marrow can rescue the high resorption phenotype in HDAC9-KO recipients. Mechanistically, this antiosteoclastogenic effect is mediated by a mutual suppression between HDAC9 and PPARγ/RANKL signaling: in the absence of RANKL, HDAC9 impedes PPARγ function by both reducing PPARγ expression and suppressing PPARγ activity via corepressors such as SMRT and NCoR; in the presence of RANKL, activation of RANKL downstream transcription factors such as NFκB and activation of PPARγ by its agonist such as rosiglitazone diminishes HDAC9 expression, leading to the recruitment coactivators and HATs and activation of PPARγ target genes (Figure 5).

HDAC inhibitors are currently used clinically to treat several diseases, including epilepsy (27, 28) and cancers (10, 29, 30). These include the Food and Drug Administration-approved valproate as an antiepileptic and anticonvulsant, vorinostat and romidepsin for the treatment of cutaneous T-cell lymphoma, as well as more than a dozen of others that are in clinical trials. Of note, HDAC inhibitors are more tolerated and effective in hematologic cancers than in solid tumors (31, 32). It is conceivable that these HDAC inhibitors may also affect other hematopoietic cell types such as osteoclasts to impact bone resorption and bone mass. Interestingly, in several human studies, long term use of broad HDAC inhibitors such as valproate has been shown to decrease BMD (33, 34). Paradoxically, in vitro studies indicate that broad HDAC inhibitors such as trichostatin A and sodium butyrate can suppress osteoclast differentiation and promote osteoblast differentiation, indicating bone-protective effects (35, 36). It is possible that individual class or member of HDACs play opposite roles in bone remodeling, for example, osteoclastogenesis has been shown to be inhibited by HDAC7 (12, 13) but enhanced by HDAC3 (12). Importantly, most of the studies to date on HDAC regulation of bone are conducted with in vitro cultures and broad-spectrum HDAC inhibitors. These approaches may distort the true HDAC functions due to the pharmacological dose used, the multitarget inhibition and the isolation from physiological context, thus making it impossible to dissect the specific physiological role of each HDAC to distinguish the friends and foes of the skeletal maintenance.

Our recent studies described here and reported in 2013 (13) have identified HDAC9 and HDAC7 as the first HDAC members that exert physiologically significant functions in the regulation of osteoclastogenesis and bone resorption. The findings that both HDAC9 and HDAC7 suppress osteoclast differentiation implicate that long-term usage of inhibitors for class IIa HDACs may risk bone loss side effects. Future studies are required to further delineate the roles of other HDAC members in bone remodeling. These efforts will ultimately facilitate the development of class/member-specific HDAC inhibitors that maintain its therapeutic benefits but minimize detrimental bone loss side effects. It is equally exciting that novel HDAC modulators may serve as potential strategies to prevent and treat bone degenerative diseases such as osteoporosis, arthritis, and bone metastasis of cancers.

Acknowledgments

We thank Dr Eric Olson and Dr Rhonda Bassel-Duby (University of Texas Southwestern) for HDAC9-KO mice, HDAC9 expression vector, and HDAC9-luc plasmid; Dr Paul Dechow and Dr Jerry Feng (Baylor College of Dentistry at Dallas) for assistance with μCT and histomorphometry analyses; and University of Texas Southwestern Biostatistics Core for assistance with statistical analyses. Y.W. is a Virginia Murchison Linthicum Scholar in Medical Research.

Address all correspondence and requests for reprints to: Yihong Wan, Department of Pharmacology, University of Texas South-

western Medical Center, 6001 Forest Park Road, Room ND9.502, Dallas, TX 75390-9041. E-mail: yihong.wan@utsouthwestern.edu.

This work was supported by the National Institutes of Health Grant R01 DK089113 (to Y.W.), the Cancer Prevention Research Institute of Texas Grant RP130145 (to Y.W.), the Department of Defense Grant W81XWH-13-1-0318 (to Y.W)., the March of Dimes Foundation Grant 6-FY13-137 (to Y.W.), The Welch Foundation Grant I-1751 (to Y.W.), and the University of Texas Southwestern Medical Center Endowed Scholar Startup Fund (Y.W.).

Disclosure Summary: The authors have nothing to disclose.

References

1. **Novack DV, Teitelbaum SL.** The osteoclast: friend or foe? *Annu Rev Pathol*. 2008;3:457–484.
2. **Teitelbaum SL.** Bone resorption by osteoclasts. *Science*. 2000; 289(5484):1504–1508.
3. **Wan Y.** PPARγ in bone homeostasis. *Trends Endocrinol Metab*. 2010;21(12):722–728.
4. **Wan Y, Chong LW, Evans RM.** PPAR-γ regulates osteoclastogenesis in mice. *Nat Med*. 2007;13(12):1496–1503.
5. **Boyle WJ, Simonet WS, Lacey DL.** Osteoclast differentiation and activation. *Nature*. 2003;423(6937):337–342.
6. **Tolar J, Teitelbaum SL, Orchard PJ.** Osteopetrosis. *N Engl J Med*. 2004;351(27):2839–2849.
7. **Lee KK, Workman JL.** Histone acetyltransferase complexes: one size doesn't fit all. *Nat Rev Mol Cell Biol*. 2007;8(4):284–295.
8. **Glass CK, Rosenfeld MG.** The coregulator exchange in transcriptional functions of nuclear receptors. *Genes Dev*. 2000;14(2):121–141.
9. **Gregoretti IV, Lee YM, Goodson HV.** Molecular evolution of the histone deacetylase family: functional implications of phylogenetic analysis. *J Mol Biol*. 2004;338(1):17–31.
10. **Johnstone RW.** Histone-deacetylase inhibitors: novel drugs for the treatment of cancer. *Nat Rev Drug Discov*. 2002;1(4):287–299.
11. **Kazantsev AG, Thompson LM.** Therapeutic application of histone deacetylase inhibitors for central nervous system disorders. *Nat Rev Drug Discov*. 2008;7(10):854–868.
12. **Pham L, Kaiser B, Romsa A, et al.** HDAC3 and HDAC7 have opposite effects on osteoclast differentiation. *J Biol Chem*. 2011; 286(14):12056–12065.
13. **Jin Z, Wei W, Dechow PC, Wan Y.** HDAC7 inhibits osteoclastogenesis by reversing RANKL-triggered β-catenin switch. *Mol Endocrinol*. 2013;27(2):325–335.
14. **Yan K, Cao Q, Reilly CM, Young NL, Garcia BA, Mishra N.** Histone deacetylase 9 deficiency protects against effector T cell-mediated systemic autoimmunity. *J Biol Chem*. 2011;286(33): 28833–28843.
15. **Cao Q, Rong S, Repa JJ, St Clair R, Parks JS, Mishra N.** Histone deacetylase 9 represses cholesterol efflux and alternatively activated macrophages in atherosclerosis development. *Arterioscler Thromb Vasc Biol*. 2014;34(9):1871–1879.
16. **Chatterjee TK, Basford JE, Knoll E, et al.** HDAC9 knockout mice are protected from adipose tissue dysfunction and systemic metabolic disease during high-fat feeding. *Diabetes*. 2014;63(1):176–187.
17. **Chatterjee TK, Idelman G, Blanco V, et al.** Histone deacetylase 9 is a negative regulator of adipogenic differentiation. *J Biol Chem*. 2011;286(31):27836–27847.
18. **International Stroke Genetics Consortium (ISGC), Wellcome Trust Case Control Consortium 2 (WTCCC2), Bellenguez C, et al.** Genome-wide association study identifies a variant in HDAC9 associated with large vessel ischemic stroke. *Nat Genet*. 2012;44(3): 328–333.
19. **Zhang CL, McKinsey TA, Chang S, Antos CL, Hill JA, Olson EN.** Class II histone deacetylases act as signal-responsive repressors of cardiac hypertrophy. *Cell*. 2002;110(4):479–488.
20. **Krzeszinski JY, Wei W, Huynh H, et al.** miR-34a blocks osteoporosis and bone metastasis by inhibiting osteoclastogenesis and Tgif2. *Nature*. 2014;512(7515):431–435.
21. **Wei W, Dutchak PA, Wang X, et al.** Fibroblast growth factor 21 promotes bone loss by potentiating the effects of peroxisome proliferator-activated receptor γ. *Proc Natl Acad Sci USA*. 2012; 109(8):3143–3148.
22. **Bai S, Kopan R, Zou W, et al.** NOTCH1 regulates osteoclastogenesis directly in osteoclast precursors and indirectly via osteoblast lineage cells. *J Biol Chem*. 2008;283(10):6509–6518.
23. **Wei W, Zeve D, Suh JM, et al.** Biphasic and dosage-dependent regulation of osteoclastogenesis by β-catenin. *Mol Cell Biol*. 2011; 31(23):4706–4719.
24. **Haberland M, Arnold MA, McAnally J, Phan D, Kim Y, Olson EN.** Regulation of HDAC9 gene expression by MEF2 establishes a negative-feedback loop in the transcriptional circuitry of muscle differentiation. *Mol Cell Biol*. 2007;27(2):518–525.
25. **Wei W, Zeve D, Wang X, et al.** Osteoclast progenitors reside in the peroxisome proliferator-activated receptor γ-expressing bone marrow cell population. *Mol Cell Biol*. 2011;31(23):4692–4705.
26. **Wei W, Wang X, Yang M, et al.** PGC1β mediates PPARγ activation of osteoclastogenesis and rosiglitazone-induced bone loss. *Cell Metab*. 2010;11(6):503–516.
27. **Miziak B, Chroscinska-Krawczyk M, Blaszczyk B, Radzik I, Czuczwar SJ.** Novel approaches to anticonvulsant drug discovery. *Expert Opin Drug Discov*. 2013;8(11):1415–1427.
28. **Marson AG, Al-Kharusi AM, Alwaidh M, et al.** The SANAD study of effectiveness of valproate, lamotrigine, or topiramate for generalised and unclassifiable epilepsy: an unblinded randomised controlled trial. *Lancet*. 2007;369(9566):1016–1026.
29. **Kumagai T, Wakimoto N, Yin D, et al.** Histone deacetylase inhibitor, suberoylanilide hydroxamic acid (Vorinostat, SAHA) profoundly inhibits the growth of human pancreatic cancer cells. *Int J Cancer*. 2007;121(3):656–665.
30. **Olsen EA, Kim YH, Kuzel TM, et al.** Phase IIb multicenter trial of vorinostat in patients with persistent, progressive, or treatment refractory cutaneous T-cell lymphoma. *J Clin Oncol*. 2007;25(21): 3109–3115.
31. **Duvic M, Talpur R, Ni X, et al.** Phase 2 trial of oral vorinostat (suberoylanilide hydroxamic acid, SAHA) for refractory cutaneous T-cell lymphoma (CTCL). *Blood*. 2007;109(1):31–39.
32. **O'Connor OA, Heaney ML, Schwartz L, et al.** Clinical experience with intravenous and oral formulations of the novel histone deacetylase inhibitor suberoylanilide hydroxamic acid in patients with advanced hematologic malignancies. *J Clin Oncol*. 2006; 24(1):166–173.
33. **Boluk A, Guzelipek M, Savli H, Temel I, Ozisik HI, Kaygusuz A.** The effect of valproate on bone mineral density in adult epileptic patients. *Pharmacol Res*. 2004;50(1):93–97.
34. **Vestergaard P, Rejnmark L, Mosekilde L.** Fracture risk associated with use of antiepileptic drugs. *Epilepsia*. 2004;45(11):1330–1337.
35. **Schroeder TM, Westendorf JJ.** Histone deacetylase inhibitors promote osteoblast maturation. *J Bone Miner Res*. 2005;20(12):2254–2263.
36. **Rahman MM, Kukita A, Kukita T, Shobuike T, Nakamura T, Kohashi O.** Two histone deacetylase inhibitors, trichostatin A and sodium butyrate, suppress differentiation into osteoclasts but not into macrophages. *Blood*. 2003;101(9):3451–3459.